Astronomy & Astrophysics manuscript no. paper2c
April 28, 2008

The structure of the inner Oort cloud from the simulation of its formation for two giga-years

G. Leto[1], M. Jakubík[2], T. Paulech[3], L. Neslušan[2], and P. A. Dybczyński[4]

[1] Catania Astrophysical Observatory, Via Santa Sofia 78, I-95123 Catania, Italy
e-mail: gle@astrct.oact.inaf.it
[2] Astronomical Institute of the Slovak Academy of Sciences, 05960 Tatranská Lomnica, Slovakia
e-mail: mjakubik@ta3.sk; ne@ta3.sk
[3] Astronomical Institute of the Slovak Academy of Sciences, Dúbravská cesta 9, 84504 Bratislava, Slovakia
e-mail: astrotom@savba.sk
[4] Astronomical Observatory of the A. Mickiewicz University, Słoneczna 36, 60-286 Poznań, Poland
e-mail: dybol@amu.edu.pl

Received April 30, 2008; accepted ???? ??, ????

ABSTRACT

Aims. Considering the model of the initial disc of planetesimals consisting of 10 038 test particles, we simulated the formation of the distant comet reservoirs for the 2 -Gyr period. The result concerning an outer part of the Oort cloud was described in our previous paper. Here, using the resultant data from the simulation, we deal with the evolution of the population and structure at 2 Gyr of the complementary inner part of the Oort cloud.
Methods. The dynamical evolution of the massless test particles was followed via numerical integration of their orbits. We considered the perturbations by four giant planets on their current orbits and with their current masses, as well as the perturbations by the Galactic tide and passing stars.
Results. The efficiency of the formation of inner OC is found to be very low: only about 1.1% of all considered particles ended in this part of the comet cloud. The particles originated from the Uranus (35.5%), Neptune (35.4%), and Edgeworth-Kuiper-belt (18.4%) regions of the initial proto-planetary disc, in particular. At 2 Gyr, the dynamics of the inner cloud is prevailingly governed by the dominant z-term of the Galactic tide. The number density of the bodies is proportional to the heliocentric distance, r, as $\propto r^{-3.53}$. The directional distributions of orbits is still strongly inhomogeneous. There are, for example, large empty regions in the space angles around the Galactic Equator points with the galactic longitude 90^o and 270^o (non-rotating frame), or there are only few bodies having the ecliptical latitude higher than $+60^o$ or lower than -60^o. A strong concentration of objects at the Ecliptic is apparent up to ≈1 000 AU (with a possible, but not exactly proved extension to ≈1 500 AU). Beyond $r \approx 6\,000$ AU, the bodies directly above and below the Sun, with respect to the Ecliptic, are absent.

Key words. Comets: general – Oort cloud – Solar system: formation

1. Introduction

Dynamically *new* comets are those observed in the zone of visibility, which were not significantly perturbed by the planets during their former revolution around the Sun. They come from the outer part of the comet Oort cloud (OC, hereinafter), which is thus observationally detectable. The researchers noticed that the original (before the entering of the planetary region) semi-major axes of new comets were not shorter than a typical down limit a_c. Hills (1981) suggested that this inner limit occurred due to an observational constraint. In the reality, the comet cloud can continually extend inward. This hypothetical part of the comet cloud, which cannot be detected by the direct observations of comets incoming from there, is referred to as *inner OC*, at the present.

In our previous work (Dybczyński et al., 2008; this work is referred to as Paper I, hereinafter), we performed a simulation of the OC formation considering the massless test particles (TPs). The approximation of real planetesimals or cometary nuclei with the massless particles allows the using of the GRID-computing technique, with a number of mutually independent CPUs, that used to be easier accessible than a supercomputer. In our Paper-I simulation, we considered the model of the initial disc of planetesimals consisting of 10 038 TPs and studied their dynamics during 1 Gyr, when influenced the perturbations by the four giant planets (on their current orbits and with their current masses), Galactic tide, and nearby passing

Send offprint requests to: L. Neslušan

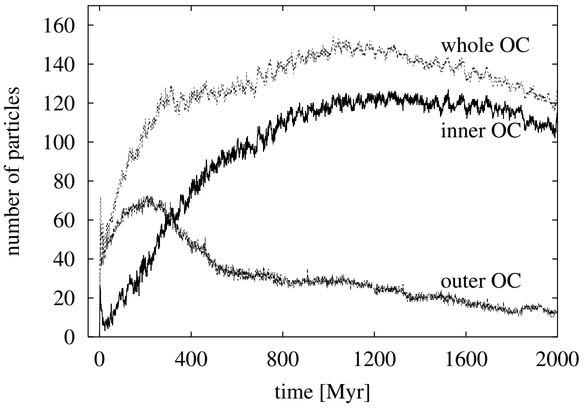

Fig. 1. The evolution of the population of the OC during the first two giga-years. The evolution of all: inner-OC, outer-OC, as well as whole-OC populations is demonstrated.

stars. A more detailed description of the initial conditions and computational procedure used can be found in Paper I, where basing on this simulation, we described the formation and some structural characteristics of the outer part of the OC.

In the present work, we again use the resultant data from the former simulation, meanwhile extended for the period of 2 Gyr, and describe the formation process, further dynamical evolution, and some features of the structure of up-to-date hypothetical inner part of the OC, which appeared in our research to form much slower than the outer one (see Fig.1).

2. The inner Oort cloud from our simulation

2.1. Introduction remarks

We classify a given TP as a member of the inner OC, if: its perihelion distance, q, is $q \geq 50$ AU and its semi-major axis, a, is $2\,000 < a \leq a_c$, whereby we put $a_c = 25\,000$ AU.

It is worthy to note that the critical semi-major axis a_c, representing the border between the inner and outer OC, is difficult to be determined by both observations and theory. It should be large enough the outer perturbers of the OC, especially the dominant and permanently acting Galactic tide, are sufficient to reduce the comet perihelia from the region beyond the relatively strong Jupiter and Saturn perturbations to the zone of visibility within a single orbit. Hills (1981) suggested $a_c = 20\,000$ AU. That time, astronomers however used to consider the value $\rho_{GM} = 0.185\,M_\odot pc^{-3}$ (Bahcall, 1984) of the Galactic-matter density. Recently, a more reliable value $\rho_{GM} \approx 0.1\,M_\odot pc^{-3}$ (Pham, 1997; Crézé et al., 1998; Holmberg & Flynn, 2000) was determined on the basis of the Hipparcos observations. It is well known: a lower ρ_{GM}, a larger a_c.

During several decades in the past, all comets having the original reciprocal semi-major axis lower than 1×10^{-4} AU^{-1} were regarded as new and, therefore, coming from the outer OC. This criterion was invalidated by Dybczyński (2001) who demonstrated that 41 of 85 comets, classified as new by the above criterion, were significantly perturbed by the planets at their previous perihelion passage. Consequently, if we want to find a characteristic border between the inner and outer OC in term of semi-major axis, which is naturally implied by a disappearance of truly new comets in observational data, we should take these facts into account and shift a_c to a larger value than that corresponding to $1/a_c = 10^{-4}$ AU^{-1} or even larger than 20 000 AU corresponding to $\rho_{GM} = 0.185\,M_\odot pc^{-3}$. In this work, we accept the result published in the recent study by Dybczyński (2006) who demonstrated that observed dynamically new comets have semi-major axes that are greater than 25 000 AU even if the $\rho_{GM} = 0.1\,M_\odot pc^{-3}$ value of the local Galactic-matter density is used.

A study of the dynamics of inner-OC bodies can be complicated by a necessity of a very long period of numerical integration of their orbits. It is well known that the dominant outer perturbation occurring due to the z-term of the Galactic tide causes the periodic variations of the orbital elements. The period of these variations is proportional to the semi-major axis as $\propto a^{-3/2}$ (Heisler & Tremaine, 1986). In contrast to the outer OC, where the periods are shorter than a giga-year, the orbital elements of the inner-OC comets can vary with a period much exceeding the age of the solar system. Due to this circumstance, we do not attempt to extrapolate our results for the period of the first two giga-years to the current inner OC. Nevertheless, the found results can still be interesting, because this first period was important for an occurrence of all charateristic evolutionary features.

2.2. Forming of the inner Oort cloud

The evolution of the inner-OC population is demonstrated in Fig. 1. The maximum population occurs at about 1 250 Myr. At the end of our simulation corresponding to the time of 2 Gyr, this population is represented by 110 TPs that implies 1.1% efficiency of the inner-OC formation. At this time, the population of the outer OC is represented only with about 13 TPs (0.13% formation efficiency). One can calculate that only 10% of the TPs, that reside in the OC, reside in its outer part at 2 *Gyr*. These figures are different from the corresponding values obtained in analogous simulations by Duncan et al. (1987) or Dones et al. (2005). However, several parameters in our models of the initial proto-planetary disc (PPD) and stellar perturbations as well as our definitions and covered time interval are different, therefore the direct comparison is impossible.

All end states at 2 Gyr are summarized in Table 1 by the region of the initial PPD, in which the TPs originated. Concerning the contributions to the inner OC from the individual regions, these contributions are 4.5%, 6.3%, 35.5%, 35.4%, and 18.4% from the Jupiter, Saturn, Uranus, Neptune, and Edgeworth-Kuiper belt (EKB, hereinafter) regions, respectively. (The evolution of these contributions is also illustrated in Fig. 2). The listed amounts are similar to those relevant to the outer OC (Paper I), besides the expected lower amount of the TPs from Jupiter-Saturn region in a comparison with the Uranus-Neptune region. The distribution of the TPs situated in the inner OC at 2 Gyr by the region of their origin is also shown in Fig. 3 (full bars). In contrast to the formation of the outer OC, a lot of TPs have come into the inner OC also from the initial heliocentric distance of 35 – 37 AU. This location corre-

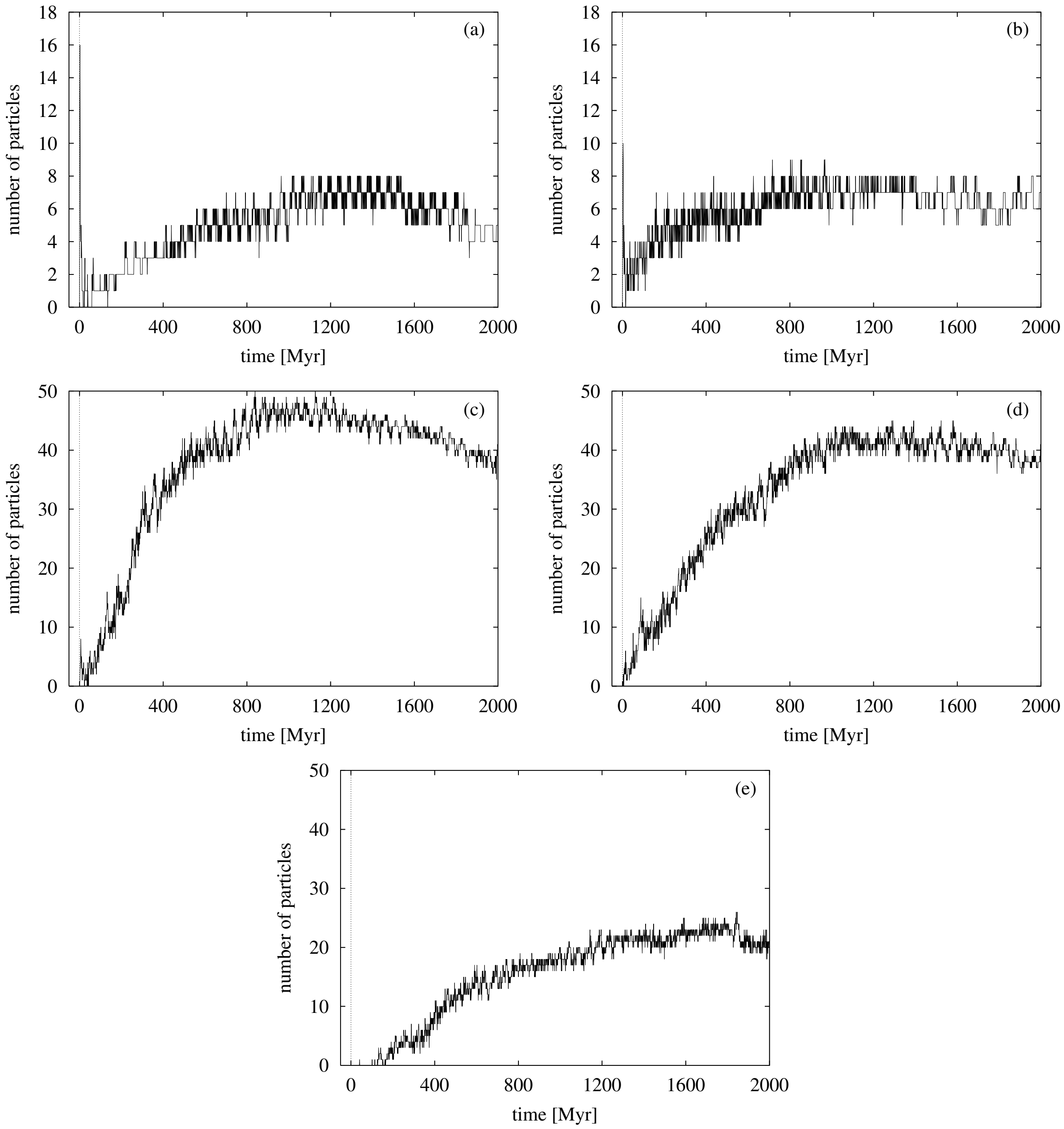

Fig. 2. The evolution of the delivery of comets to the inner OC, which initially originated in the Jupiter (a), Saturn (b), Uranus (c), Neptune (d), and EKB (e) regions. Notice the different vertical scale.

sponds with the 4:3 mean-motion resonance with Neptune. The transiting population of bodies, which have occurred sometime during the 2 Gyr evolution in the inner OC, is illustrated with the empty bars in Fig. 3.

2.3. The radial structure of the inner OC

The cumulative distribution and radial distribution of the TPs in several selected moments are illustrated in Fig. 4 and 5, respectively. To see these inner-OC distributions in a wider context, we plot the cumulative distribution function for 100 – 100 000 AU interval and the radial distribution for the entire studied region from 0 to 100 000 AU. At 2 Gyr, the number of TPs increases in the highest rate with heliocentric distance in the interval from $\approx$ 3 000 to $\approx$ 25 000 AU (Fig. 4), i.e. in almost whole region of the inner OC, in particular. The behaviour of the radial distribution of TPs in the inner cloud is rather chaotic during an early stage of its formation (Fig. 5a-d). Only when the inner-OC population approaches its maximum, at $\approx$ 1 250 Myr, and after the maximum, the inner cloud becomes more and more centrally concentrated. At 2 Gyr, the number density of the TPs residing in the OC in the interval $5\,000 < r < 100\,000$ AU can be fitted by the power law with the index of slope $s = -3.529^{+0.031}_{-0.024}$. (The corresponding behaviour of the heliocentric-distance distribution is illustrated with the solid curve in Fig. 5f). This value is almost consistent, within the determination uncertainty, with $s = -3.5$ found by Duncan et al. (1987) for 3 000 – 50 000 AU interval, but at 4.5 Gyr.

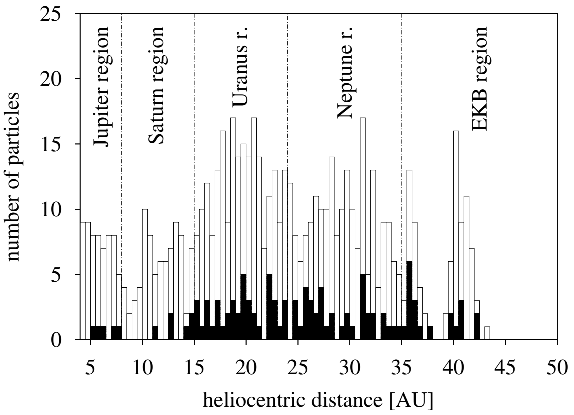

Fig. 3. The numbers of the TPs moved into the inner OC from the Jupiter, Saturn, Uranus, Neptune, and Edgeworth-Kuiper-belt regions. The full bars illustrate the numbers of the TPs in 0.5 AU-wide intervals of the initial PPD, which reside in the inner OC at 2 Gyr. The empty bars do so for the TPs ever occurring, at least for a short period, in the inner OC. (The animation of the evolution of this dependence during the entire investigated period is available, in the *avi* format, on: http//www.ta3.sk/˜mjakubik/AstroDyn/INNER_OC_FORMATION.)

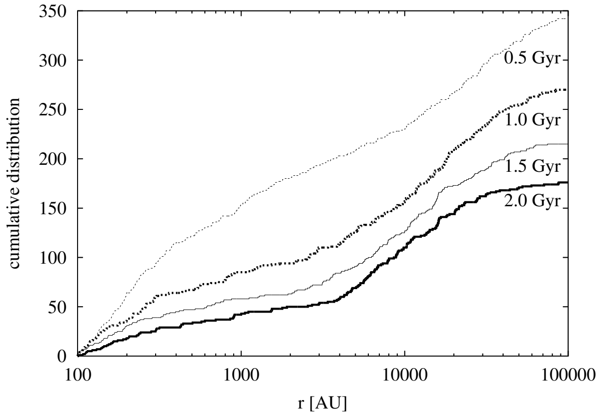

Fig. 4. The cumulative distribution of the TPs after 500, 1000, 1500, and 2000 Myr. (The animation of the evolution of this dependence during the entire investigated period is available, in the *avi* format, on: http//www.ta3.sk/˜mjakubik/AstroDyn/INNER_OC_FORMATION.)

Table 1. The end states, at 2 Gyr, of the TPs, which resided in various regions (the first column) of the PPD in the beginning of performed simulation. In the beginning, we consider the PPD consisting of 10 038 TPs. In the end of the simulation some of the TPs, from the given part of planetary region, still have their perihelion, q, in this region, i.e. $q < 50$ AU, or they are moved into the inner (IOC) or outer (OOC) Oort cloud, *ejected* into the interstellar space, or were destroyed at a *collision* with one of the considered massive bodies, mostly with the Sun. An asterisk indicates the average values from the period 1991−2000 Myr, since the numbers still vary, in the these cases.

region	$q < 50$	in IOC*	in OOC*	ejected	collided
Jupiter	50	4.9	2.0	1389	187
Saturn	13	6.9	1.0	1802	260
Uranus	62	39.0	3.3	1596	367
Neptune	173	38.9	3.0	1443	390
EKB	1734	20.2	3.3	439	122

In Fig. 6, we show the distribution of semi-major axis of the TPs, which are situated in the OC at 2 Gyr. Again, we deal with a larger than the inner-OC interval of a and demonstrate, in particular, a smooth transition from the inner to outer part of the comet cloud. The a-distribution also evidences the centrally concentrated OC. (A decrease in the inner-most interval of 0 – 5 000 AU is caused by the existence of the inner limit of the cloud due to its definition, not by a lack of TPs.) The behaviour in the 5 000 – 50 000 AU interval can be approximated by the power law with the index $s_a = -1.736^{+0.038}_{-0.028}$.

The information contained in the distribution of the semi-major axis is completed with the information being in the distribution of eccentricity of the inner-OC orbits at 2 Gyr, which can be seen in Fig. 7. At 2 Gyr, a prevailing part of TPs in the inner OC moves on highly eccentric orbits. One can notice that the eccentricities lower than about 0.2 are missing. The animation of the entire evolution of this distribution (*fig07.avi*) confirms an expected fact that the TPs come to the inner OC on highly eccentric orbits, with $e \rightarrow 1$. Due to the periodic variation of this element, which is coupled with the periodic variation of the perihelion distance at an almost constant semi-major axis, some values of e lower than 0.98 begin to appear after 30 Myr. Then, the lower and lower values of the eccentricity start to appear. The down limit of ≈ 0.2 is reached after about 500 Myr. During the 500 – 2 000 Myr period, the values lower than 0.2 also occur, but only sporadically and for a short time. The typical distribution during this period is similar to that at 2 Gyr, shown in Fig. 7.

2.4. The orientation of the inner-OC orbits

In our computation, we used the non-rotating galactic coordinate frame, whereby its initial orientation was chosen to be identical to its current orientation. In the presented figures, we still use this orientation enabling a simple transformation between the galactic and ecliptic coordinate systems. This fact is necessary to be kept in the mind if one wanted to relate a structure to the position of the Galactic centre or solar apex, which are uncertain in the given context. To indicate the difference between the used and regular galactic frames, we refer the used frame as ”zero-time galactic coordinate frame”, hereinafter.

In Fig. 8, there are demonstrated the distributions of angular orbital elements of the TPs, which stay in the inner OC at the end of the simulation (at 2 Gyr), in both zero-time-galactic and ecliptical coordinate systems. Because of a relatively small numerousity of the TPs in the inner OC at the given time, the height of the bars in the plots slightly varies, when the plots are constructed for several, not very different times (e.g. 1 960, 1 980, 2 000 Myr). However, in all such mutually corresponding plots, we can see, in the zero-time galactic coordinates (left-column plots): (i) a very hight peak at $80^o \lessapprox i \lessapprox 90^o$ and the zero-value or close-to-zero-value minima at $i \lessapprox 55^o$ and $i \gtrapprox 100^o$ in plot (a) (see also animation *fig08a.avi*), (ii) the maxima at $90^o - 180^o$ and $260^o - 320^o$ intervals and minima at $0^o - 60^o$ and $180^o - 220^o$ intervals in plot (c), and (iii) the high maximum in $160^o - 180^o$ interval (a wider maximum in $140^o - 200^o$) and minimum in $220^o - 340^o$ interval in plot (e).

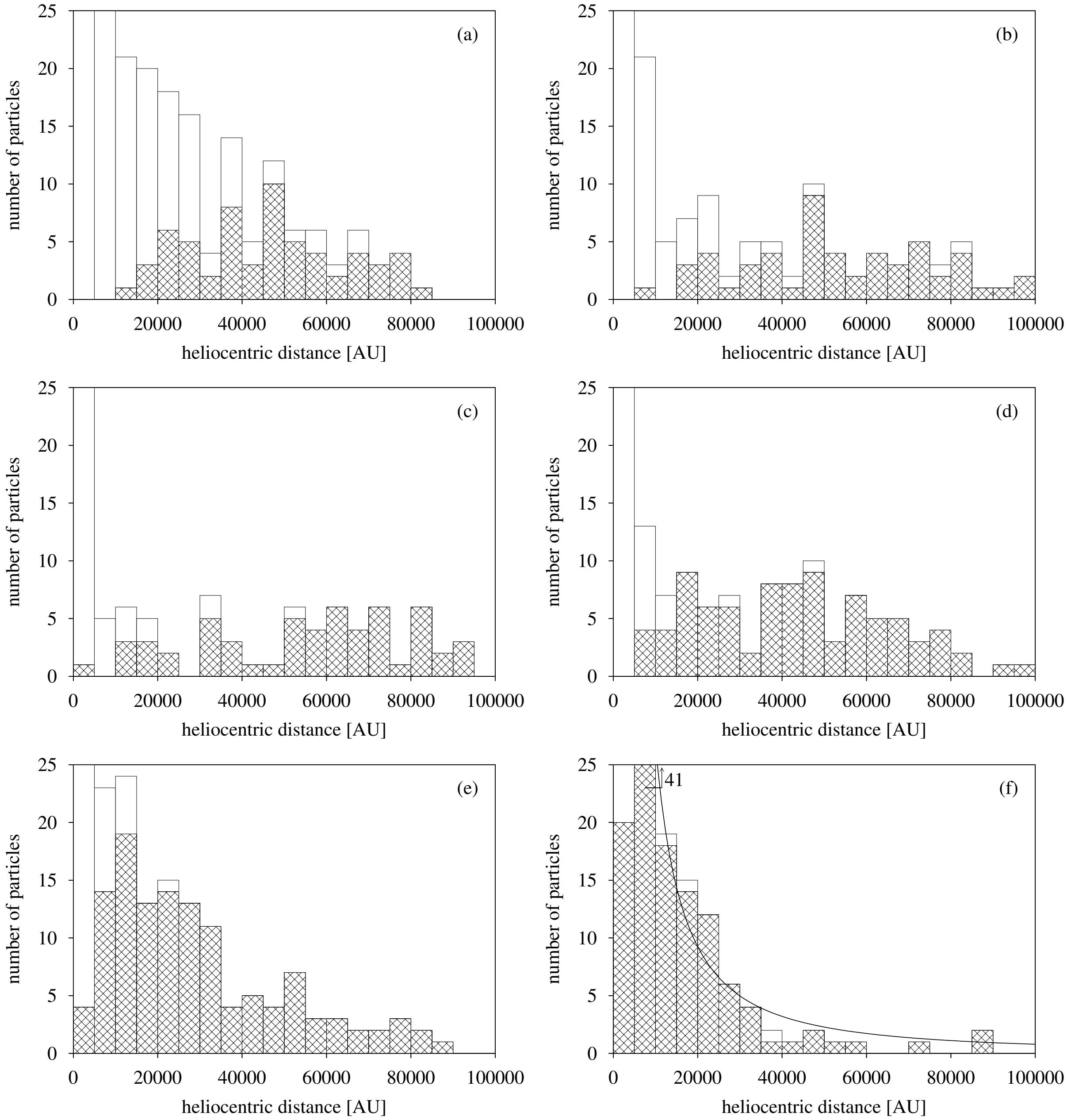

Fig. 5. The distribution of the heliocentric distance of OC comets (crosshatched bars) for the times of 2 (plot a), 8 (b), 31 (c), 125 (d), 500 (e), and 2 000 Myr (f). The corresponding distributions of all comets, still bound to the Sun, are also shown (empty bars). In the region $r < 10\,000$ AU, the second distributions are outside of the chosen scale because of a better transparency of the first group of distributions (in plot f, the bar for $5\,000 < r < 10\,000$ AU is also out of the range; the actual value is given as numeral). If all comets in the given interval are in the OC, the crosshatched bar overlaps the empty bar, which is not visible in this interval, then. In plot f, our fit of the behaviour in the interval from 5 000 to 100 000 AU, by the power-law with index $s = -1.53$, is shown with the solid curve. (The animation of the evolution of this distribution during the entire investigated period is available, in the *avi* format, on: http//www.ta3.sk/˜mjakubik/AstroDyn/INNER_OC_FORMATION.)

The corresponding features can be seen in the distributions constructed in the ecliptical coordinate system (right-column plots of Fig. 8). Seeing the plot showing the ecliptical distribution of the argument of perihelion, ω_e, (Fig. 8d) or the corresponding animation (*fig08c.avi*) from ≈ 300 Myr, the maxima in this distribution are related to the initial values in quadrants, approximately, centred at 0^o and 180^o, in which the perihelia of the largest number of TPs were detached from the planetary region by the Galactic tide. Another information about the directional distribution of bodies in the inner OC can be deduced from Fig. 9 illustrating the directions of their aphelion points as well as from Fig. 10 giving the positions of some orbital elements in the dependence on the semi-major axis.

All plots in Figs. 8 and 9 document the expected scenario of the formation of OC inner part. At the beginning (see also animation *fig09b.avi*), the comets are delivered to the inner OC on orbits with a very low inclination to the Ecliptic. The Galactic tide is mostly efficient when acting on the orbits with the aphe-

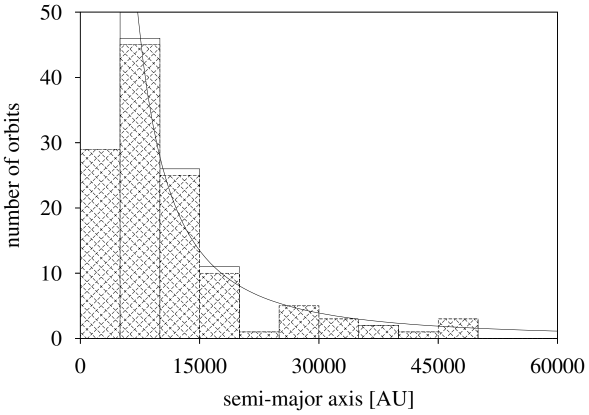

Fig. 6. The distribution of the orbital semi-major axis of TPs residing in the OC at 2 Gyr (crosshatched bars). The corresponding distribution of all comets, still bound to the Sun, is also shown (empty bars). In the interval from 5 000 to 50 000 AU, the inner-OC semi-major-axis distribution is fitted by the power law with the index of slope $s_a = -1.74$ (solid curve). (The animation of the evolution of this distribution during the entire investigated period is available, in the *avi* format, on: http//www.ta3.sk/˜mjakubik/AstroDyn/INNER_OC_FORMATION.)

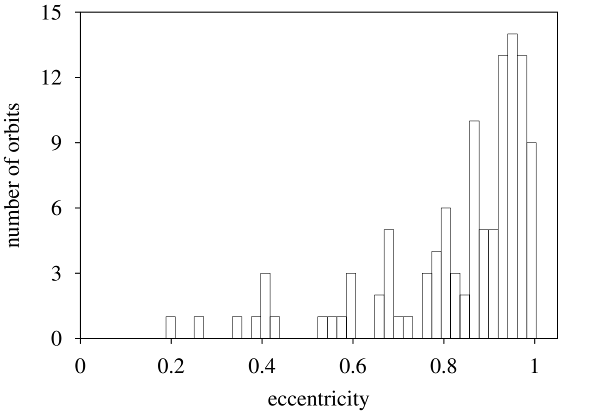

Fig. 7. The distribution of the orbital eccentricity of TPs residing in the inner OC at 2 Gyr. (The animation of the evolution of this distribution during the entire investigated period is available, in the *avi* format, on: http//www.ta3.sk/˜mjakubik/AstroDyn/INNER_OC_FORMATION.)

lia in large distances (also large angular distances) from the Galactic-Equator plane (Galactic z-component of the aphelion point is large). So, these orbits are soon changed by the tide. The tide is less efficient in the case of comets approaching the inner OC on orbits with the aphelia in a vicinity of the Galactic-equator plane. Here, the process of their change is relatively slow. Some orbits with a low inclination to both Ecliptic and Galactic Equator can be seen surviving in a relatively low galactic-latitude region ($-45^o < b < +45^o$) in Fig. 9a. In the range of b between approximately -45^o and $+45^o$ far from the Ecliptic, there are almost no aphelia.

We suggest that there is no sufficient mechanism to change the orbits in the way their aphelia would appear in this interval of b far from the Ecliptic. The secondary outer perturbers are, probably, too weak to change the orbits so much. Analyzing this absence of the aphelia as well as the absence of aphelia above the ecliptic latitude $\beta = +60^o$ and below $\beta = -60^o$, approximately (Fig. 9b), we can take into account and deduce the following. The dominant z-term of the Galactic tide is known to cause the cyclic change of Galactic inclination only from a limiting (mostly different from 90^o) value to a value approaching 90^o in the same quadrant as the limiting value. We know that the variation of the galactic inclination is coupled with that of the perihelion distance, whereby the inclination approaches its limiting value just in the moment, when the perihelion distance is in the minimum of its periodic-variation cycle. This is also the case, when the TPs are escaping from the planetary region. Let us stress here that such escape is due to the planetary perturbations only, which cause the semi-major axis (and consequently the aphelion distance) to grow enough to allow the Galactic tide do start its action (but leaving the perihelion distance mostly unchanged). At this point the inclination to the Ecliptic is still small. Thus, a TP starting its moving to the inner OC should be on an orbit with the galactic inclination close to the limiting value. At the same time, the inclination to the Ecliptic, which is inclined to the Galactic Equator by 60.2^o, is very low. Thus, the galactic inclination can typically librate only within the interval from the limiting value, being close to 60^o, to 90^o. In the ecliptic coordinate frame, the inclination can vary, due to the described mechanism, from 0^o to $\approx 30^o$ resulting in the ecliptic-latitude variation of the aphelion points from roughly -30^o to $+30^o$. This implies a certain significance of the secondary outer perturbers, too, since we observe (Fig. 9b) also some aphelia in the intervals of β from $+30^o$ to $+60^o$ and from -60^o to -30^o, approximately.

As mentioned in Paper I, the Galactic inclination of orbits with the very short perihelia in the minimum of the libration cycle of this element approaches the value of 90^o for a relatively long period due to the action of the dominant, z-term of Galactic tide. Therefore, the probability of the occurrence of an orbit with a very high Galactic inclination is high. This can explain the high peak in the interval of $80^o - 90^o$ in Fig. 8a (or in the interval $25^o - 35^o$ in Fig. 8b, with respect to the angle between the Ecliptic and Galactic-Equator planes).

In the case of inner OC, the magnitudes of the action of outer perturbers are weaker than the corresponding magnitudes in the case of outer OC. It is, therefore, not surprising that the described distributions of the orbital elements of the TPs situated in the inner OC imply a large inhomogenity in the structure of the whole part of this cloud even after 2 Gyr lasting evolution. In 2 Gyr, the inhomogenity is, however, not longer caused by the origin of the TPs in a flat PPD. The initial dynamical memory is forgotten and the actual dynamics is governed, in particular, by the dominant, z-term of the Galactic tide. Though the outer perturbers are inefficient to completely thermalize even the most distant part of the inner OC, they seem to be efficient enough to significantly change a prevailing part of its orbits.

At the end of this subsection, let us to ask how are all the characteristics of the inner OC found for the end of our simulation at 2 Gyr related to the current structure of this part of the comet cloud? Can the largest periods of element variations of the inner-most orbits in the inner OC, not covered by our simulation, cause some significant differences between the overall

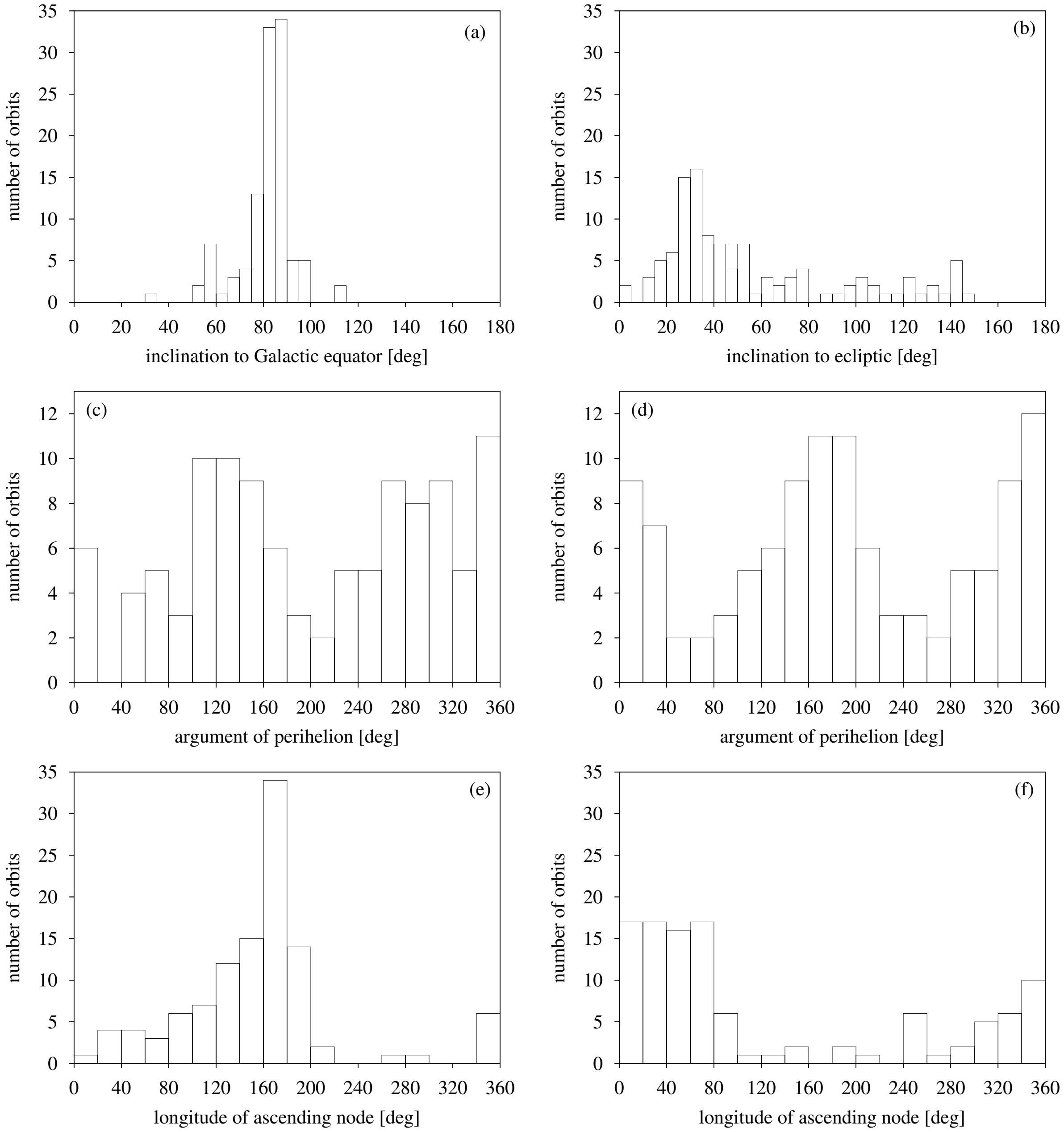

Fig. 8. The distributions of angular elements of TPs residing in the inner OC at 2 Gyr. The left-column plots demonstrate the distributions in the zero-time galactic coordinate frame, the right-column plots in the ecliptic coordinate frame. The pairs of plots (a)-(b), (c)-(d), and (e)-(f) demonstrate the distribution of the inclination (to the Galactic plane or to the Ecliptic), argument of perihelion, and longitude of ascending node, respectively. Notice the different vertical scale. (The animations of the evolution of these distributions during the entire investigated period are available, in the *avi* format, on: http//www.ta3.sk/˜mjakubik/AstroDyn/INNER_OC_FORMATION.)

pictures of this part of OC at 2 Gyr and at the present? In the related animations (*fig05.avi–fig12b.avi*), the general features, which can be seen, are more or less conserved from the time of about 1 250 Myr, when the population of the inner OC reached its maximum. The period from 1 250 to 2 000 Myr is, however, relatively short, therefore it would be risky to extrapolate the result from this period to the whole subsequent period from 2 Gyr till the present (4.5 Gyr). Though a radical change of the inner-OC structure can hardly be expected, yet, we cannot exclude a quantitative change due to a slow, but permanent dynamical evolution.

2.5. The flatteness of the trans-Neptunian belt and inner OC

No empty regions exist between the populations of small bodies beyond the orbit of Neptune. The division into the EKB, scattered disc, extended scattered disc, and inner OC is established only for our methodological purpose. The trans-Neptunian disc, containing the objects on orbits with a low inclination to the Ecliptic, is expected to smoothly expand into a less and less flat region and gradually become a spherical comet cloud. In this subsection, we attempt, on the basis of

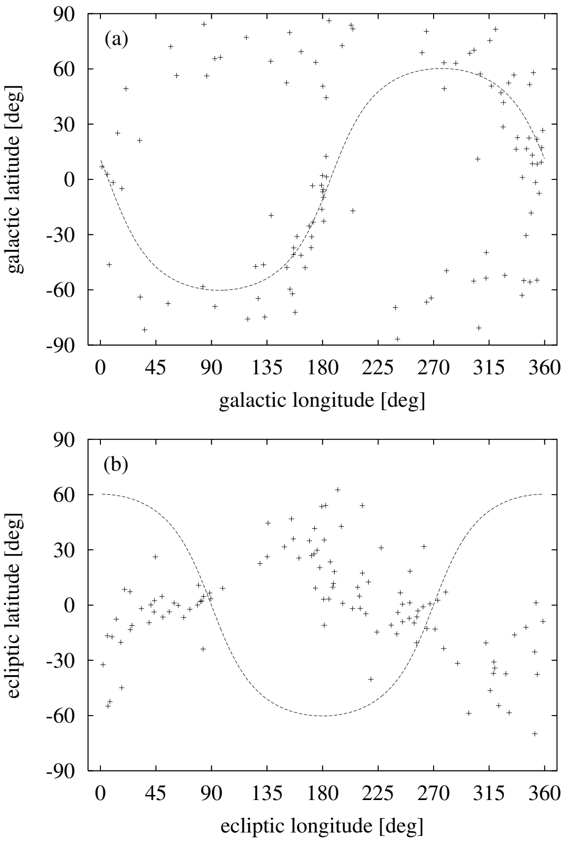

Fig. 9. The directional distribution of the aphelion points of TPs residing in the inner Oort cloud at 2 Gyr. Plot (a) demonstrates the distribution in the zero-time galactic coordinate frame, plot (b) does this in the ecliptic coordinate frame. The dashed curve shows the position of the Ecliptic in plot (a) and Galactic Equator in plot (b). (The animations of the evolution of these distributions during the entire investigated period are available, in the *avi* format, on: http//www.ta3.sk/~mjakubik/AstroDyn/INNER_OC_FORMATION.)

our simulation, to answer the question of how quickly the low inclination of the disc-object orbits to the Ecliptic disappears and at what heliocentric distance the more or less spherically symmetric comet cloud occurs.

We know that the orbits of bodies in the EKB have a low inclination to the Ecliptic (typically up to 40^o). Our question on the flatteness of trans-Neptunian population concerns the more distant regions, in particular. The distribution of the TPs, having their semi-major axes in the interval $50 < a < 25\,000$ AU in the $i - a$ phase space, is illustrated in Fig. 11. (More exactly, the upper a in the upper plot is 22 000 AU, since there is no TP with a between 20 490 and 25 280 AU.) We can see that the larger and larger values of the inclination occur with the increasing semi-major axis. The PPD departures, step by step, from the Ecliptic. The inclinations larger than $\approx 45^o$ occur for $a \gtrapprox 4\,000$ AU and those larger than $\approx 90^o$ for $a \gtrapprox 8\,500$ AU.

An interesting phenomenon is an almost disappearance of the TPs with $i \lessapprox 20^o$ for $a \gtrapprox 5\,500$ AU. This phenomenon likely occurs due to the geometry of the initial appearance of bodies in the inner OC and very long periods of the variation of inclination in this part of the OC. The bodies are delivered there on a close-to-zero inclination to the Ecliptic. This value corresponding to the minimum of the inclination libration cycle caused by the Galactic tide is changed relatively quickly in a first stage (newly coming bodies move only a short time on orbits with $i \to 0^o$), but very slowly later. The time of 2 Gyr (or shorter at later incoming to the inner OC) appears to be too short to complete the entire libration cycle and return the inclination below the value of 20^o.

For $a \gtrapprox 10\,000$ AU, the inclination to the Ecliptic fills the entire interval from $\approx 20^o$ to $\approx 150^o$. However, it does not exceed $\approx 150^o$ even at the outer border of the inner OC. The reason of this phenomenon is obviously the same as that discussed in the description of Fig. 9 in Sect. 2.4. The absence of orbits with the ecliptical $i \gtrapprox 150^o$ and $i \lessapprox 20^o$ (the latter for $a \gtrapprox 5\,500$ AU) implies that the inner OC is not spherically symmetric in any part, and this fact does not allow to perform a more exact evaluation of the trans-Neptunian disc flatteness, with the more exactly determined characteristics.

The spatial flatteness of the trans-Neptunian disc can better be seen in the distribution of the ecliptical z-component of the TPs at the final time of the simulation (Fig. 12). Unfortunately, there are not very large numbers of the TPs in the critical intervals of heliocentric distance, r, in which the flatteness starts to disappear. Seeing a more central region $r < 5\,000$ AU (Fig. 12b), we can conclude that the part of the disc in the region of $r \lessapprox 1\,000$ AU is clearly situated nearly the Ecliptic. Beyond this (but possible $r \approx 1\,500$ AU) distance, more TPs are situated at a larger distance from the Ecliptic. The magnitude of TPs' z-component seems to fill the whole interval from 0 to r only in the region between $3\,000 \lessapprox r \lessapprox 6\,000$ AU, therefore our simulation does not exclude a disc that could, practically, be spherically symmetric in this interval (but it does not either prove the symmetry due to a poor statistics). Beyond $r \approx 6\,000$ AU, the TPs situated directly above and below the Sun (with respect to the Ecliptic) are missing. This absence is obviously linked to the absence of orbits with $i \gtrapprox 150^o$.

3. Summary and discussion

Considering the model of the PPD consisting of 10 038 TPs and perturbations by four giant planets on their current orbits and with their current masses, as well as the perturbations by the Galactic tide and passing stars, we simulated the formation of the OC and the accompanying dynamical evolution of the Edgeworth-Kuiper belt for the period of 2 Gyr. In this paper, we dealt with the inner OC, in particular. For the last 0.75-Gyr period, the general structure of the inner OC and adjacent regions does not significantly change, but one must be careful when extrapolating the structure for 2 Gyr to the present cloud. Though slowly, it has still evolved during another 2.5 Gyr, therefore some differences could appear.

The inner-OC population quickly rises during the first mega-year due to the ejections of TPs from the Jupiter-Saturn region (Fig. 1). However, after reaching a very early maximum, it steeply decreases. From few mega-years after the beginning, it again increases more or less linearly, with a high slope, untill about 500 Myr. Also after this time, the practically linear increase continues, but with a lower slope, till the maximum at

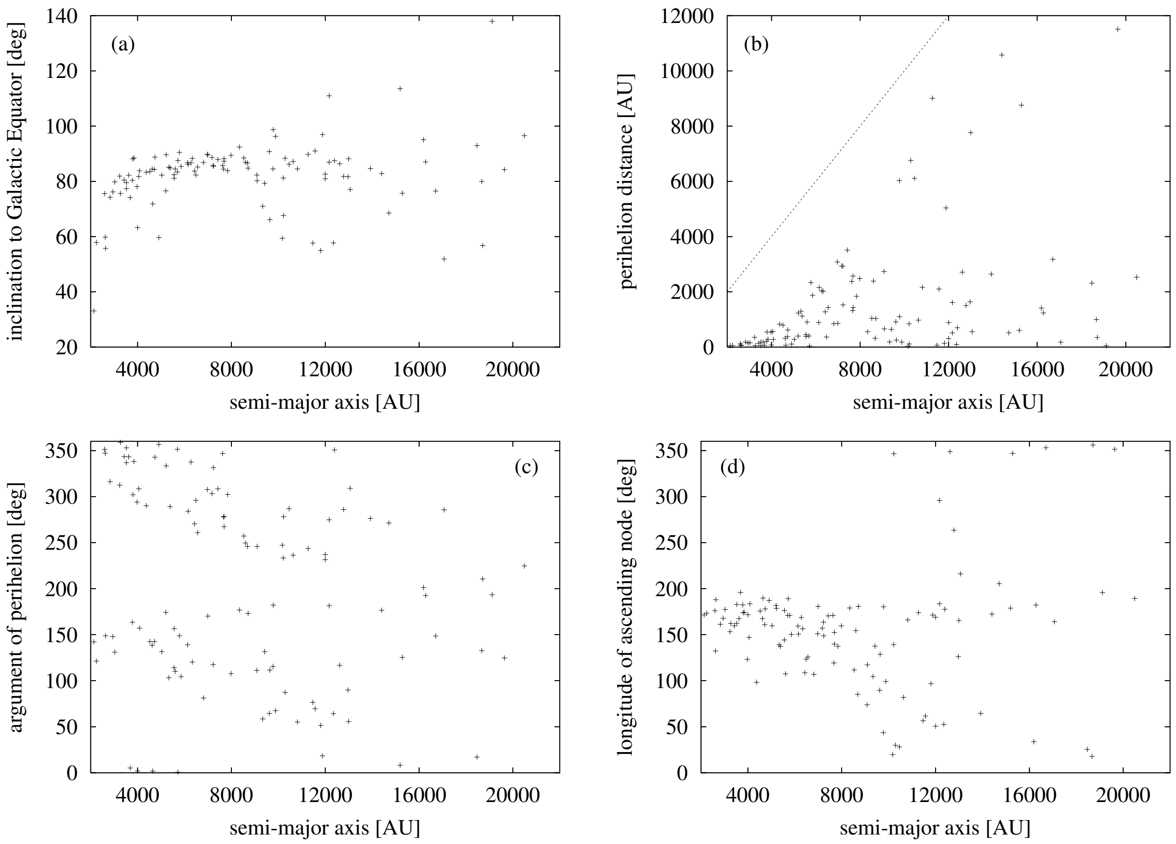

Fig. 10. The inclination to the Galactic Equator (a), perihelion distance (b), zero-time-galactic argument of perihelion (c), and zero-time-galactic longitude of ascending node (d) of the TPs residing in the inner OC at 2 Gyr as the functions of their semi-major axis. The phase-space above the straight line in plot (b) is forbidden. (The animations of the evolution of these plots during the entire investigated period are available, in the *avi* format, on: http//www.ta3.sk/~mjakubik/AstroDyn/INNER_OC_FORMATION.)

about 1 250 Myr. Dividing the TPs in the inner OC by the region of their origin, we can conclude that the largest amounts originate from the Uranus and Neptune regions: 35.5% and 35.4%, respectively. The amount of the TPs originating in the EKB region appears to be larger than each of the amounts from the Jupiter and Saturn regions from $\approx$ 500 Myr, and clearly exceeds these amounts at 2 Gyr. At this time, there are 4.5%, 6.3%, and 18.4% TPs originating in the Jupiter, Saturn, and EKB regions, respectively, in the inner OC.

According our simulation and definitions of the inner and outer OC, only about 10% of the TPs, that are in the OC at 2 Gyr, reside in the outer OC. The formation efficiency of the inner OC is 1.1%. So, it is lower than the corresponding values obtained by previous authors for the present epoch or 4 Gyr (Duncan et al. (1987) obtained $\approx$ 20%; Dones et al. (2005) obtained 2.7% in their *cold* and 3.5% in their *hot run* for the inner OC). Because of the assumption of different initial parameters in the considered models and different definitions used by the authors, a direct comparison of the results as well as an analysis of the causes of differences are impossible.

At 2 Gyr, the number density of the TPs residing in the OC in the interval $5\,000 < r < 100\,000$ AU can be fitted by the power law with the index of slope $s = -3.529^{+0.031}_{-0.024}$. Within the determination uncertainty, this value of slope index is consistent with $s = -3.5$, which was found by Duncan et al. (1987) for the interval of $3\,000 < r < 100\,000$ AU and time 4.5 Gyr. The distribution of the semi-major axis in the 5 000−50 000 AU interval can also be approximated by the power law with the index $s_a = -1.736^{+0.038}_{-0.028}$. The distribution of eccentricity of the inner-OC orbits implies that a prevailing part of TPs in the inner OC move on highly eccentric orbits. The eccentricities lower than about 0.2 are almost missing.

Even after 2-Gyr evolution, the orientation of the inner-OC orbits is strongly inhomogeneous. The inhomogenity can be seen in the distributions of the zero-time-galactic angular elements (Fig. 8). Specifically, there is a very hight peak at $80^o \lessapprox i \lessapprox 90^o$ and the zero-value or close-to-zero-value minima at $i \lessapprox 55^o$ and $i \gtrapprox 100^o$ (see also animation *fig08a.avi*) in the distribution of inclination. Further, we can see the maxima at $90^o - 180^o$ and $260^o - 320^o$ intervals and minima at $0^o - 60^o$ and $180^o - 220^o$ intervals in the distribution of the argument of perihelion. And, the distribution of the longitude of ascending node has a high maximum in $160^o - 180^o$ interval and minimum in $220^o - 340^o$ interval. The corresponding features can also be seen in the distributions constructed in the ecliptical coordinate system. The inclination to the Ecliptic fills the entire interval from $\approx 20^o$ to $\approx 150^o$, for $a \gtrapprox 10\,000$ AU. However, it does not exceed the value of $\approx 150^o$ even at the outer border of the inner OC. The inhomogenity is also apparent from the plots of the directional distributions of aphelion points (Fig. 9). There are

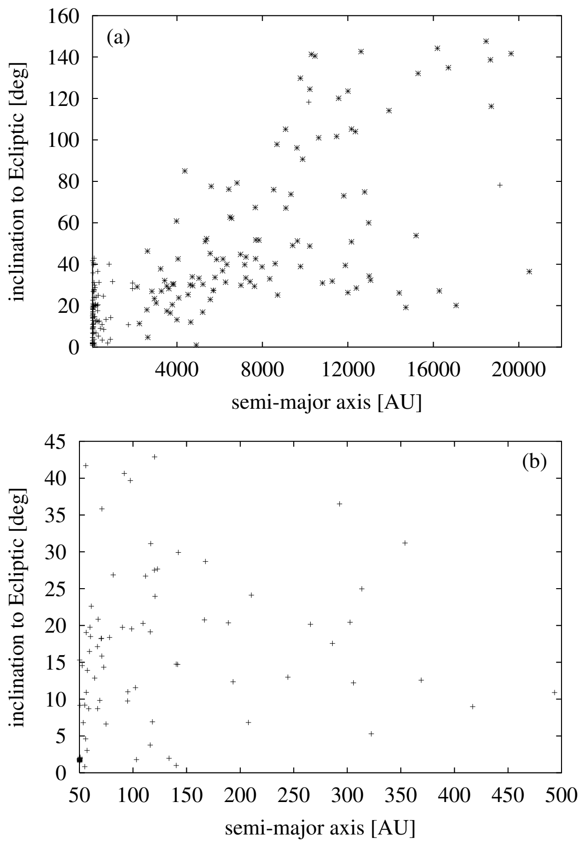

Fig. 11. The inclination to the Ecliptic vs. semi-major axis of the TPs on the orbits with semi-major axis in the interval $50 < a < 22\,000$ AU (a) and $50 < a < 500$ AU (b) at 2 Gyr. The TPs residing in this time in the inner OC are shown with asterisks, the other TPs with crosses. (The animations of the evolution of plot (a) as well as the more detailed view in plot (b) during the entire investigated period are available, in the *avi* format, on: http//www.ta3.sk/~mjakubik/AstroDyn/INNER_OC_FORMATION.)

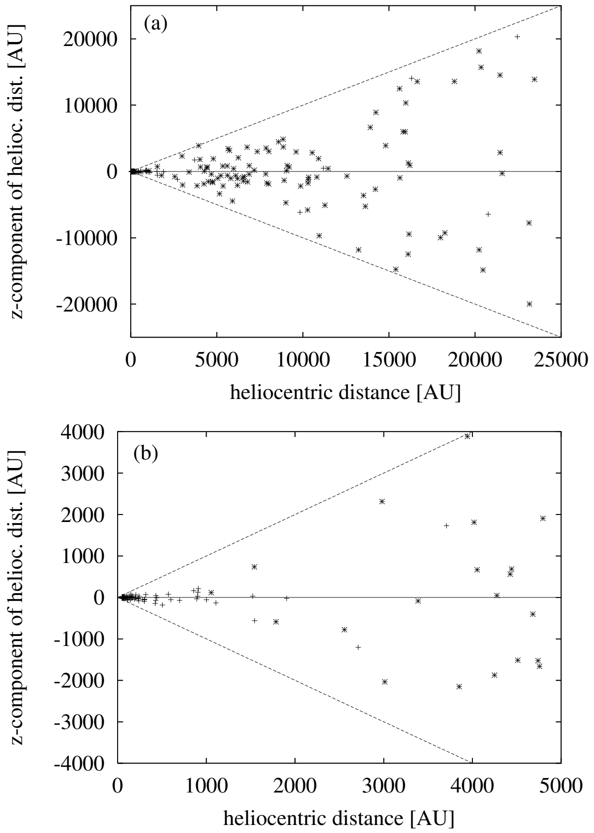

Fig. 12. The occurrence the TPs above and below the Ecliptic. Specifically, the ecliptical z-component of heliocentric distance vs. this distance of the TPs is shown, at 2 Gyr. In more detail, the TPs up to outer border of the inner OC are demonstrated. Plot (a) demonstrates the z vs. r distribution for $50 < r < 25\,000$ AU and plot (b) is a more detailed view of the $50 < r < 5\,000$ AU interval. The TPs residing at 2 Gyr in the inner OC are shown with asterisks, the other TPs with crosses. Since $|z| \leq r$, no TP can occur above the upper and below the down diagonals. (The animations of the evolution of plot (a) as well as the detailed view in plot (b) during the entire investigated period are available, in the *avi* format, on: http//www.ta3.sk/~mjakubik/AstroDyn/INNER_OC_FORMATION.)

quite large empty regions around the Galactic-Equator points with the longitude of 90^o and 270^o. And, almost no aphelia can be seen in an ecliptical latitude higher than $+60^o$ or lower than -60^o, approximately. At 2 Gyr, the described inhomogenity is not, however, caused by the origin of the TPs in a flat PPD. The initial dynamical memory is forgotten and the actual dynamics is governed by the dominant, z-term of the Galactic tide, in particular.

The orbits in the inner-most part of inner OC have a low inclination to the Ecliptic as expected. With respect to the semi-major axis, the inclinations larger than $\approx 45^o$ occur for $a \gtrapprox 4\,000$ AU and those larger than $\approx 90^o$ for $a \gtrapprox 8\,500$ AU. The actual location of the TP position near the Ecliptic (low magnitude of ecliptical z-coordinate) is apparent in the interval of heliocentric distance up to $\approx 1\,000$ AU. Beyond the distance of $\approx 6\,000$ AU, the TPs are also abundant at the large distances from the Ecliptic, except of the region directly above and below the Sun, with respect to the Ecliptic.

The electronic form of output data from the numerical integration of TP orbits, recorded every mega-year of the dynamical evolution, is available on: http//www.ta3.sk/~mjakubik/AstroDyn/INNER_OC_FORMATION/ for the period from 1 to 2 Gyr. The animations of the evolution of distributions plotted in Figs. 3 to 12, for the entire period from 0 to 2 Gyr, are also available on this web site. The output data for the period from 0 to 1 Gyr are available on the web page http//www.ta3.sk/~ne/OUTER_OC_FORMATION/ linked to Paper I.

Acknowledgements. G.L. thanks PI2S2 Project managed by the Consorzio COMETA, http://www.pi2s2.it and http://www.consorzio-cometa.it for the computational resources and technical support. M.J., T.P., and L.N. thank the project "Enabling Grids for E-scienE II" (http://www.eu-egee.org/) for the provided computational capacity and support in a development of the computer code, which was necessary for a management of tasks on the GRID. They also acknowledge the partial support of this work by VEGA – the Slovak Grant Agency for Science (grant No. 7047).

References

Crézé, M., Chereul, E., Bienaymé, O., & Pichon, C. 1998, A&A 329, 920
Dones, L., Weissman, P.R., Levison, H.F., & Duncan, M.J. 2004, in: Comets II, eds. M. C. Festou, H. U. Keller, and H. A. Weaver (Arizona: Univ. Arizona Press), p. 153
Dones, L., Levison, H.F., Duncan, M.J., & Weissman, P.R. 2005, private communication
Duncan, M., Quinn, T., & Tremaine, S. 1987, AJ 94, 1330
Dybczyński, P.A. 2001, A&A 375, 643
Dybczyński, P.A. 2006, A&A 449, 1233
Dybczyński, P.A., Leto, G., Jakubík, M., Paulech, T., & Neslušan, L. 2008, A&A, submitted (Paper I)
Heisler, J., & Tremaine, S. 1986, Icarus 65, 13
Hills, J.G. 1981, AJ 86, 1730
Holmberg, J., & Flynn, C. 2000, MNRAS 313, 209
Pham, H.A. 1997, in: Hipparcos Venice 97, ESA-SP 402, eds. M. A. C. Perryman and P. L. Bernaca (Noordwijk: ESA), p. 559